Fracturing and Testing Case Study of Paludal, Tight, Lenticular Gas Sands

N.R. Warpinski, SPE, Sandia Natl. Laboratories
P.T. Branagan, CER Corp.
A.R. Sattler, SPE, Sandia Natl. Laboratories
J.C. Lorenz, Sandia Natl. Laboratories
D.A. Northrop, SPE, Sandia Natl. Laboratories
R.L. Mann, SPE, CER Corp.
K.-H. Frohne, SPE, U.S. DOE

SPE 13876

Summary. This paper is a case study of the stimulation and testing of tight, lenticular sands in the paludal interval of the Mesaverde group in the Piceance basin at DOE's Multiwell Experiment (MWX) site in Colorado. Topics discussed include geologic data, stress test results, well testing, laboratory core studies, stimulation and stimulation analyses, and postfracture operations.

Introduction

For a number of years, the U.S. government has engaged in research to enhance gas recovery from unconventional reservoirs, such as organically rich, fractured shale and discontinuous, lenticular, tight sandstones. Although large quantities of natural gas are trapped in these formations, the permeabilities are too low to permit economic recovery by conventional technology. In the western U.S., the Greater Green River, Piceance, Wind River, and Uinta basins have been identified as containing significant amounts of gas in thick sections of lenticular sands. The Natl. Petroleum Council has appraised[1] these four basins to hold 136 Tcf [4×10^{12} m^3] of maximum recoverable gas in lenticular reservoirs. This sizeable resource is being investigated by the DOE in the Piceance basin of western Colorado, where a field laboratory containing three closely spaced wells penetrating the lenticular Mesaverde formation has been constructed. This facility, near Rifle, CO, is the site of the DOE MWX, which has been developed to determine the viability of the lenticular, tight sands as a gas resource.

Massive hydraulic fracturing has demonstrably increased gas production from tight reservoirs. Its performance in lenticular formations is currently unpredictable, however, because of poor definition of reservoir properties and sizes, inadequate understanding of the physics that control fracture propagation and proppant transport, limited ability to measure, describe, or evaluate the created fracture, and uncertainty as to the relationship of stimulation design variables (fluids, proppants, and pumping rates) to the resultant fracture. These difficulties are compounded in the lenticular formations by the uncertainty concerning whether multiple lenses, some remote from the wellbore, can be stimulated by a common treatment. Improved understanding, evaluation, prediction, and possible control of stimulation technology are needed for effective development of tight, lenticular reservoirs.

In this paper, we describe a case study of the testing and fracturing of lenticular sands in the paludal interval[2] of the Mesaverde group. Results include (1) geologic studies that delineate the sizes and shapes of the lenses, (2) detailed core and log reservoir/rock property data, (3) stress test data showing the vertical distribution of the horizontal in-situ stress, (4) well tests[3] (drawdown, buildup, and interference) to determine in-situ reservoir properties, (5) laboratory data[4] on fracture fluid invasion and damage, and (6) the various analytic and diagnostic[5] techniques used to evaluate the hydraulic-fracture treatment.

Overview

The objectives of this paludal experiment were to characterize the lenticular sandstones for reservoir quality and size, to determine fracture geometry and behavior in a lenticular environment, and to stimulate lenticular sandstones in this complex, coal-bearing interval successfully. To achieve these objectives, the hydraulic-fracture treatment was divided into two phases. The first phase consisted of two minifractures and step-rate/flowback tests, during which several diagnostic techniques were used to map fracture behavior. These tests also provided fracture design information for the main treatment. Associated with this phase were pre- and postfracture well tests, stress tests, and laboratory fluid-damage tests. The second phase was the full-scale treatment, again with several diagnostic techniques. Associated testing included postfracture cleanup and well tests, as well as laboratory damage and residue measurements. Detailed core and log analyses were performed to support all tests. The results of these experiments and the conclusions inferred from them will be outlined in this paper.

MWX Site

The MWX site consists of three closely spaced wells. (Wells MWX-1, MWX-2, and MWX-3). We have taken over 4,100 ft [1250 m] of core with more than 1,100 ft [335 m] of oriented, and have performed comprehensive core and log analysis programs, detailed geophysical surveys, and extensive well testing and stress testing programs. The three wells are 115 to 215 ft [35 to 66 m] apart and their depths are 8,350, 8,300, and 7,565 ft [2545, 2530, and 2306 m], respectively. The Mesaverde group at this location is found at 4,100 to 8,300 ft [1250 to 2530 m].

Geologic and Sedimentologic Setting

The paludal interval[2] refers to the Late Cretaceous lower delta plain deposits of the Williams Fork formation of the Mesaverde group. It is characterized by muddy and carbonaceous flood-plain deposits, within which narrow distributary channels, channel margin (levee) deposits, and splay (flood) deposits are interbedded. Distributary deposits typically are thick sandstones with few or no shale breaks; channel margin deposits contain thinner sandstone beds with frequent siltstone and mudstone interfingering; splay deposits are often reservoir-quality, clean sandstones near their apex (the channel) but become interbedded with siltstone and mudstone near their extremities; flood-plain deposits consist primarily of coals and mudstones.

Lorenz[2] statistically estimated the widths (narrow, horizontal channel dimension) of the sand reservoirs on the basis of two procedures. The first procedure[6] combined the correlation percentages of reservoir sandstones between the three wells with the spacing of the wells to predict an average lens width. With this procedure, lens widths for this delta plain environment are on the order of 100 to 500 ft [30 to 152 m]. The second procedure relies on the rela-

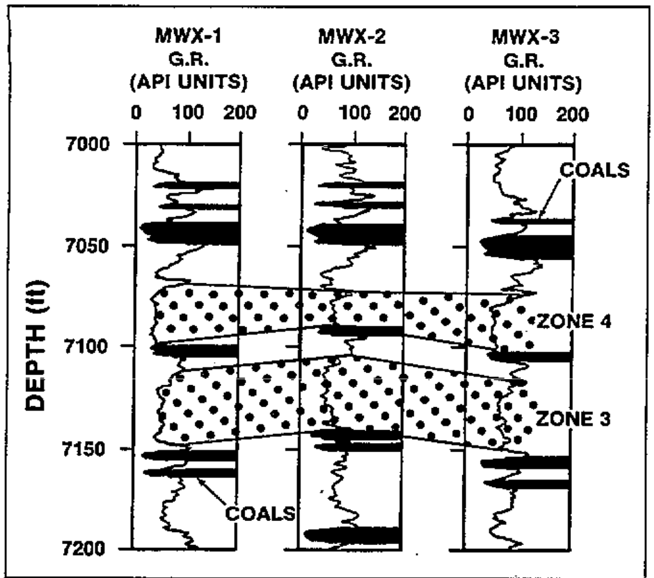

Fig. 1—Paludal Zones 3 and 4.

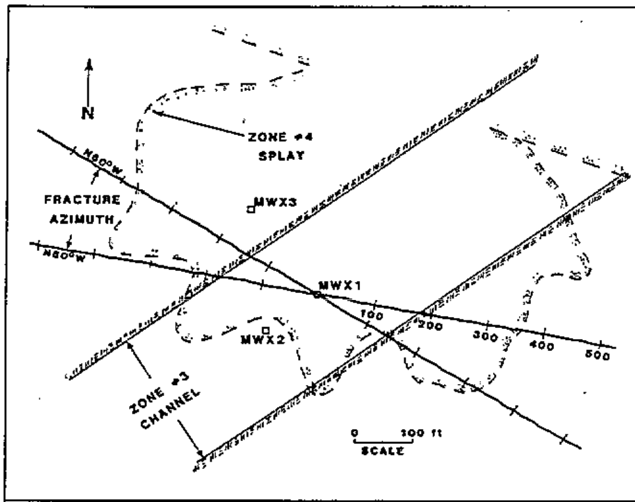

Fig. 2—Plan view of sand reservoirs and hydraulic fracture.

tionship between lens thickness (vertical dimension) and maximum lens width as measured in outcrop. A best-fit straight line through an ensemble of outcrop data yielded width=8.6 thickness$^{1.1}$, with a correlation coefficient of 0.62. Major sources of error are the scatter in outcrop data and the uncertainty of penetrating the lens in the location of its maximum width. In the 11 channel lenses encountered in MWX, the predicted widths were 80 to 550 ft [25 to 168 m]. Channel lengths are estimated to be at least one order of magnitude greater than the widths. No method is available to estimate the size of the splay deposits.

Lorenz also estimates the orientation of the channels on the basis of paleogeography, well-to-well correlations, crossbeds in oriented core, and a high-resolution dipmeter. Paleogeography suggests that the major flow direction was generally east-northeast, and most of the distributary lenses at MWX are in this range.

Fig. 1 shows correlated gamma ray logs of the two sandstone reservoirs that were chosen for hydraulic fracture. These reservoirs are labeled Zone 3, which is interpreted as a distributary channel, and Zone 4, which is interpreted as a splay deposit. Zone 3 was perforated from 7,120 to 7,144 ft [2170 to 2177 m] and Zone 4 from 7,076 to 7,100 ft [2157 to 2164 m]. Zone 3 is probably about 350 ft [107 m] wide on the basis of its 28-ft [8.5-m] thickness, and probably is oriented east-northeast because it intersects Wells MWX-1 and MWX-2, but is only marginally evident in Well MWX-3. No size estimates are available for Zone 4 (because it is a splay), but the splay probably originated from a channel to the north-northeast because this zone is thick in Wells MWX-1 and MWX-3 but is marginal in Well MWX-2.

Fig. 2 shows a plan view of this representation of Zones 3 and 4. Also shown is the expected hydraulic-fracture azimuth from several stress-orientation measurement techniques.[7] The probable intersection of the hydraulic fracture and the sand reservoirs is 200 to 500 ft [61 to 152 m], depending on the true orientation of the channel and the width of the splay.

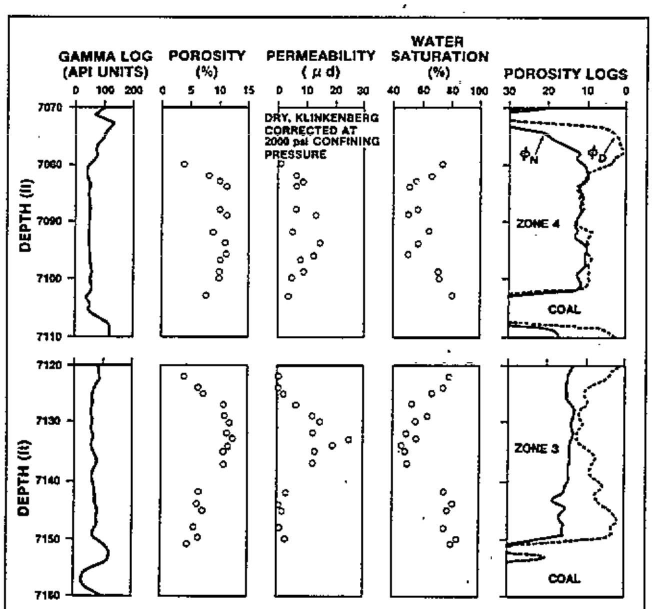

Fig. 3—Well MWX-3 core data.

TABLE 1—PALUDAL CORE DATA IN WELL MWX-3

Log Depth (ft)	Porosity (%)	Water Saturation (%)	Klinkenburg Permeability (md) At Effective Confining Stress (psi) 1,000	2,000	3,000
7,080	3.8	74	0.0020	0.0006	0.0001
7,082	8.3	66	0.0118	0.0065	0.0046
7,083	10.0	56	0.0203	0.0086	0.0063
7,085	11.1	51	0.0419	0.0062	0.0150
7,088	10.0	57	0.0101	0.0062	0.0051
7,089	11.2	51	0.0161	0.0130	0.0096
7,092	8.9	62	0.0062	0.0051	0.0037
7,094	10.8	57	0.0182	0.0144	0.0083
7,096	10.9	50	0.0165	0.0117	0.0080
7,097	10.0	50	0.0107	0.0080	0.0057
7,099	10.0	73	0.0201	0.0089	0.0060
7,100	9.8	75	0.0104	0.0053	0.0048
7,103	7.6	80	0.0072	0.0038	0.0014
7,122	4.0	86	0.0009	0.0003	0.0002
7,124	6.4	74	0.0017	0.0006	0.0003
7,125	7.1	67	0.0056	0.0021	0.0010
7,127	10.6	53	0.0154	0.0066	0.0063
7,129	10.9	64	0.0133	0.0124	0.0091
7,130	11.6	56	0.0166	0.0152	0.0136
7,132	11.4	48	0.0147	0.0128	0.0088
7,133	12.4	56	0.0323	0.0252	0.0218
7,134	11.5	45	0.0259	0.0189	0.0163
7,135	10.9	45	0.0140	0.0131	0.0115
7,137	10.8	48	0.0139	0.0123	0.0094
7,142	6.5	77	0.0053	0.0029	0.0011
7,144	6.1	80	0.0023	0.0005	0.0003
7,145	7.0	78	0.0031	0.0018	0.0010
7,148	5.6	76	0.0041	0.0011	0.0009
7,150	6.4	84	0.0032	0.0028	0.0010
7,151	4.6	81	0.0021	0.0004	0.0002

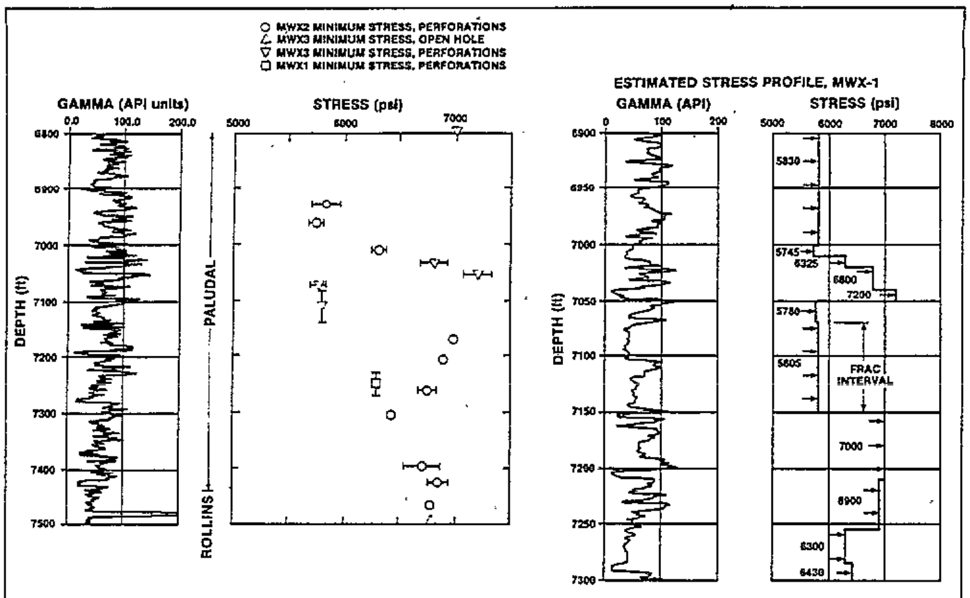

Fig. 4—Stress data and estimated stress profile in Well MWX-1.

One other factor further complicates this geometry. A fault with a 12-ft [4-m] throw intersects Well MWX-2 just above Zone 4. The orientation of this fault is not known, but it does not intersect the other wells. It is assumed that it is oriented in the same direction as the natural fractures observed in oriented core, about N70°W.

The final complication is the presence of coal beds above, below, and in between Zones 3 and 4. The proximity of these coals to the reservoir sands was a cause for concern in designing the fracture treatments.

Core and Log Analyses

Core was obtained in both zones in Wells MWX-2 and MWX-3. None of it was oriented in this interval. Fig. 3 and Table 1 show an example of the results of special core analyses including Boyles law porosity measurements, dry, Klinkenberg-corrected permeability measurements at confining stress (2,000 psi [14 MPa]), and water saturation, S_w, data. Also shown for correlation are the gamma and porosity logs. In this well, Well MWX-3, a casual look at the logs shows little developed porosity. However, the 10 to 12% porosity measured in core in these zones was the best in the entire Mesaverde section (see Table 1). Dry, Klinkenberg-corrected permeabilities of 10 to 20 μd were also the highest matrix permeabilities measured in the section. Relative permeability data from Randolph[8] show that the gas permeabilities are a factor of 3 to 5 lower at 40% S_w and will be effectively shut off for $S_w > 60\%$. He also found that these paludal rocks are not very stress-sensitive.

Log analyses by Kukal[9] gave permeability/height, kh, values of 0.5 to 1.0 md-ft [1.5×10^{-4} to 3.0×10^{-4} md·m] for both sands in all wells, with the exception of Zone 4 in Well MWX-2, which was not analyzed for permeability. He calculated water saturations of 52 to 60% for these zones (again with the exception of Zone 4 in Well MWX-2, which was 76%).

The decreased porosity and permeability in the bottom half of Zone 3 indicate that Well MWX-3 has penetrated the channel near the margin. While the top of the zone is a clean sand (as seen in the core), the bottom shows interfingering with siltstone and mudstones and thus poor reservoir quality. These large changes in reservoir quality are typical of these lenticular reservoirs.

Several natural fractures were observed in the core (not oriented), but they were mostly in the fine-grained, thin-bedded materials, and all were calcite-filled. The televiewer log picked up seven possible fractures, but no preferred orientation of these fractures was found.

Rock properties determined from core compression tests under confining pressure resulted in a Young's modulus of about 3.7×10^6 psi [25 GPa] and a Poisson's ratio of 0.22. Poisson's ratio measured in situ with a long-spaced sonic log resulted in values of 0.16 to 0.2. Young's modulus in the bounding mudstones and siltstones was considerably greater than in the sands; values ranged from 4×10^6 to 6×10^6 psi [28 to 41 GPa]. Poisson's ratio in these rocks varied from 0.2 to 0.26. Sonic data in the bounding materials were generally unusable because of the presence of coals.

Geophysical Surveys

While a three-dimensional (3D) seismic survey, two vertical seismic profiles (one azimuthal), and two cross-well seismic surveys have been performed for this experiment,[10] the presence of coal in this interval made these data useless for any interpretation of structure and lens morphology. The coals acted as the strongest reflectors in this section and as diffraction gratings to some extent, thus masking all other important features.

Stress Test Data

In-situ stress measurements were performed throughout the paludal section to determine the vertical distribution of the minimum horizontal principal in-situ stress for hydraulic-fracture containment analyses. These measurements used the hydraulic fracturing technique as described in Ref. 11. Fig. 4 shows the minimum stress data from all three wells vs. the depth in Well MWX-2, where most of the measurements were made. Additionally, Fig. 4 shows our best reconstruction of a stress profile for Well MWX-1, the well that was stimulated. This profile is only an approximation because of the limited number of data points and the good possibility of stress variations in lateral directions.

Fig. 4 shows that we were fortunate to be located in low-stress sands with high-stress bounding layers. The upper bounding zone is fairly thin, however, and thus would not be a complete barrier to fracture propagation if the treatment pressures became high. Above this barrier, only low stresses were measured up to 6,800 ft [2073 m]; with so few data points, however, high-stress layers are still quite likely above 7,000 ft [2134 m].

The highest stress measured in the paludal section was in the coal above Zone 4 at 7,050 ft [2149 m] with a 1.02-psi/ft [23-kPa/m] gradient. Sands typically have 0.82- to 0.87-psi/ft [18.5- to 19.7-kPa/m] gradients. Of all the stress measurements performed in these wells, the data in this paludal section are the least accurate and reproducible. We believe it is a result of the complex lithology in this section; core logs show that lithologic changes are found from every few feet to as little as every few inches. Thus, a stress measurement probably "averages" these stresses, and different results should be expected for different volumes. Typical accuracies for these data are only ±50 to 100 psi [±345 to 690 kPa] for most tests.

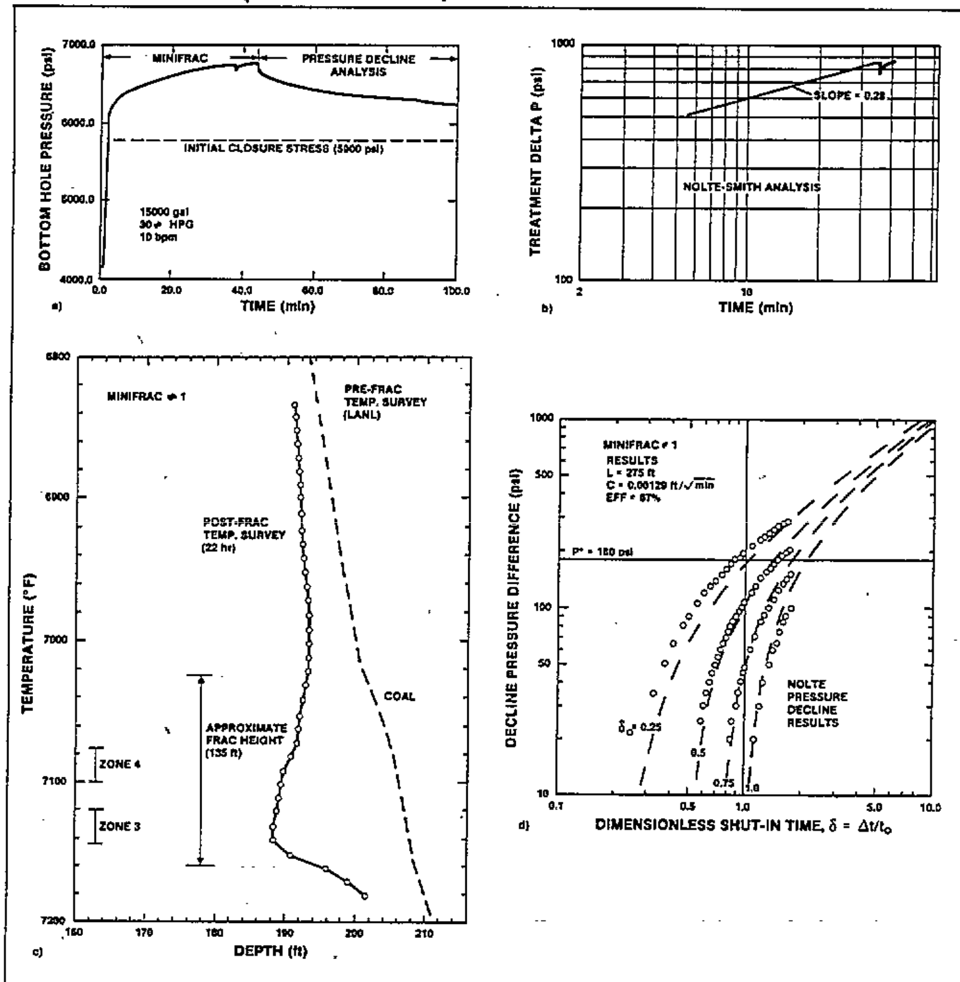

Fig. 5—Results of Minifracture 1.

Prefracture Well Test Data

Prefracture well testing[3] of commingled Zones 3 and 4 was conducted in Fall 1983. Testing consisted of an initial flow period for cleanup followed by a short buildup test and then an extended interference test. During a 7-day flow period of the interference test, the well produced at 200 to 250 Mcf/D [5665 to 7080 m^3/d] at surface pressures of 800 to 2,800 psi [5.5 to 19.3 MPa]. However, no interference was seen in the observation wells at distances of only 112 and 189 ft [34 and 58 m]. The flow period was followed by a 7-day buildup from which an initial *kh* of 0.95 md-ft [0.0003 md·m] was calculated for both zones. This yields an estimated average permeability of 36 μd, and the formation temperature was about 210°F [99°C].

The high permeability and absolute open flow (AOF) compared to the core data show that these zones are naturally fractured. Because there was no evidence of linear flow in the well test data, we are probably dealing with a fairly interconnected natural-fracture system. However, no well-to-well interference was observed with these permeabilities. For a 0.95-md-ft [0.0003-md·m] formation flowing at 250 Mcf/D [7,080 m^3/d], interference should have been observed in 1 or 2 days. The lack of interference may indicate that there is no connection between the natural fractures intersecting individual wells, and the natural fracture system is suggested to be one of subparallel fractures with low-angle intersections.[12] Other factors confusing the results are the fault in Well MWX-2 and the limited thickness of Zone 3 in Well MWX-3 (the channel margin).

Phase 1 Minifractures

The purpose of the Phase 1 minifractures was two-fold: to attempt to map fracture behavior in a lenticular reservoir by use of two minifractures with different volumes and to obtain design information for the main treatment. The approach was to conduct one small, unpropped minifracture and try to map its important characteristics, and then to conduct a second minifracture with twice the volume. We would like to discern any differences in fracture behavior or geometry that might be attributable to the lens morphology and associated stress and lithologic features. Because we were using no proppant in these tests, we could maximize our information by obtaining careful pressure-decline data after the treatment for a Nolte-type analysis.[13] Additionally, we conducted step-rate/flowback and pump-in/flowback tests before conducting the minifractures to obtain additional closure stress data that were averaged over the commingled zones. This series of tests was conducted in Well MWX-1 in Dec. 1983.

Step-Rate, Pump-In, and Flowback Tests. Step-rate/flowback and pump-in/flowback tests with KCl water were conducted to provide a suitably averaged (over the fracture size) initial closure stress for the minifracture analyses and an initial fracture extension pressure for comparison with later data should anomalous behavior occur. The step-rate test resulted in a minimum fracture extension pressure of about 5,950 psi [41 MPa]. The flowback test following the step-rate test resulted in an apparent closure stress of 5,900 psi [40.7 MPa]. The second flowback test yielded an apparent closure stress of 6,100 psi [42 MPa], considerably higher than the first test. This change in closure stress was initially attributed to leakoff of fracture fluid into the near-fracture pore space (back stress), but other interpretations are also possible. The injection pressures were 6,355 psi [43.8 MPa] bottomhole at 8 bbl/min [0.021 m^3/s] for the step-rate test and 6,500 psi [44.8 MPa] at 10 bbl/min [0.026 m^3/s] for the pump-in test (~120 bbl [19 m^3] total volume for each test). These values are quite high for pumping KCl water at these low rates. The closure stress data can be compared with a minimum

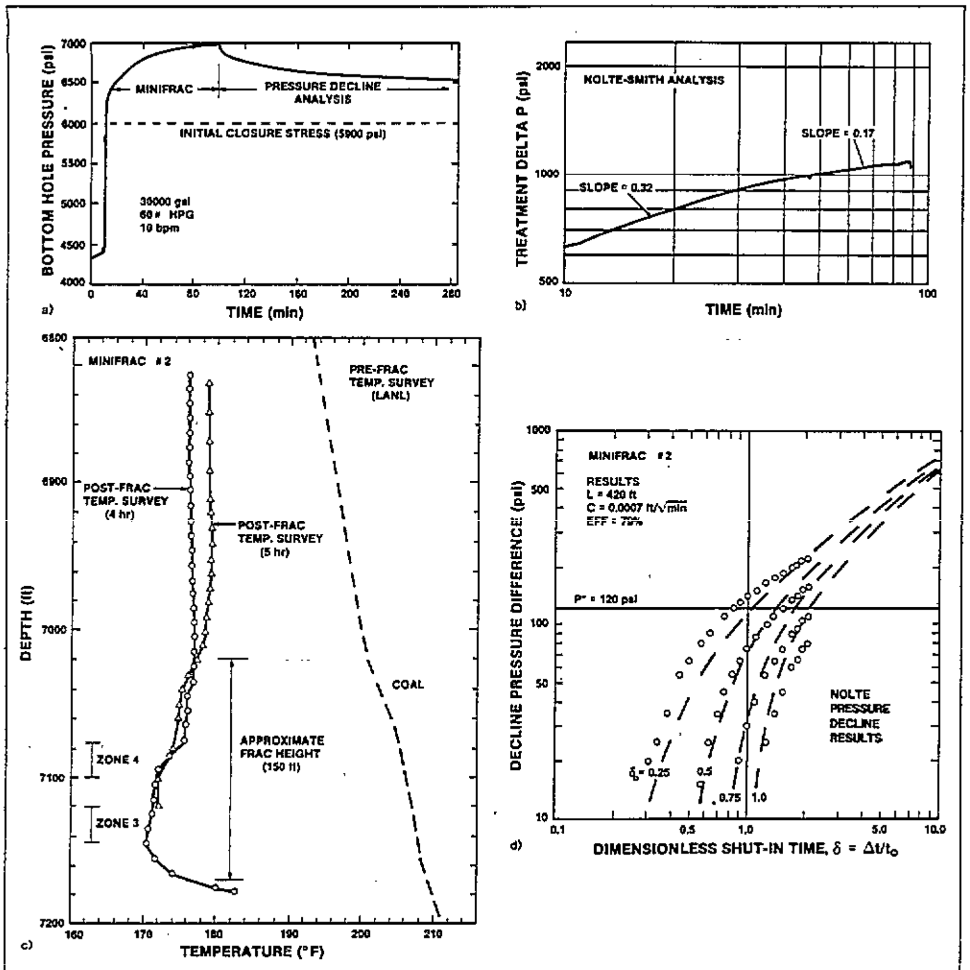

Fig. 6—Results of Minifracture 2.

stress of 5,805 psi [40 MPa] measured with a small breakdown in Well MWX-3.

Minifracture 1. Minifracture 1 was designed to be 200 ft [61 m] long so that the fracture would remain, for the most part, within the sand bodies. A volume of 15,000 gal [57 m^3] of a noncross-linked 30-lbm/1,000-gal [3.6-kg/m^3] WGA-2 gel was chosen on the basis of both pseudo-3D analyses using the measured in-situ stresses (Fig. 4) and an estimated maximum fracture height of 120 ft [37 m] (constant-height model) using the same stress data. Smith Energy Services, the stimulation contractor, suggested a prepad of low-pH methanol to reduce formation damage and to aid fluid recovery; 2,100 gal [8 m^3] was used. This was based on a laboratory study of MWX core that showed a near 100% permeability recovery with this prepad as opposed to 40 to 60% damage for short-term data with no prepad. The flow rate was 10 bbl/min [0.026 m^3/s].

During the minifractures (as well as the step-rate/flowback tests), diagnostics consisted of the following.

1. A quartz-crystal-oscillator, bottomhole pressure (BHP) transducer, and a bottomhole temperature gauge at 6,700 ft [2042 m] in Well MWX-1 (the stimulation well) on a wireline in tubing, recording at the surface.
2. Borehole seismic geophones[5] in Wells MWX-2 and MWX-3 to map fracture geometry.
3. A postfracture temperature survey.

This treatment was conducted as planned, and the important data are shown in Fig. 5.

Fig. 5a shows the treatment pressure vs. time for this treatment. The important aspect of this figure is the high treatment pressure (800 psi [5.5 MPa] above initial closure stress). The Nolte-Smith[14] log/log plot of pressure behavior (Fig. 5b) yields an exponent of 0.28, which is higher than the value of 0.22 expected for a fluid with this rheology (n'=0.76; k'=0.00072 lbf-sec$^{n'}$/ft^2 [0.034N·s$^{n'}$/m^2]). Nevertheless, the plot indicates that the fracture was extending in length without excessive height growth. The temperature log in Fig. 5c indicates that total fracture height was on the order of 135 ft [41 m], although the top of the fracture is equivocal. The Nolte pressure-decline analysis[13] (Fig. 5d), using a height of 135 ft [41 m], a plane-strain modulus of about 4.5×10^6 psi [31 GPa], a viscosity degradation exponent of 1.0, a leakoff height of 55 ft [16.8 m], a pump time of 43 minutes, and an instantaneous shut-in pressure (ISIP) of 6,670 psi [46 MPa], results in a wing length of 275 ft [84 m] and a leakoff coefficient of 0.0013 ft/$\sqrt{\text{min}}$ [0.0004 m/$\sqrt{\text{min}}$]. These results are longer than the design, but this is probably a result of neglecting the methanol prepad in the design calculations and calculating a lower gross leakoff coefficient than used in the design. Two shut-ins during the treatment were analyzed following Nierode[15] and resulted in a leakoff coefficient less than 0.001 ft/$\sqrt{\text{min}}$ [0.0003 m/$\sqrt{\text{min}}$]. Results of the borehole seismic geophones will be given in a later section.

Minifracture 2. Minifracture 2 was designed to be twice the size of Minifracture 1 and used 30,000 gal [114 m^3] of a noncross-linked 60-lbm/1,000-gal [7.2-kg/m^3] WGA-2 gel, a more viscous fluid. A 4,500-gal [17-m^3] prepad of low-pH methanol was again used, and the flow rate for this test was also 10 bbl/min [0.027 m^3/s]. The same diagnostics were used to evaluate fracture behavior.

The data from Minifracture 2 are shown in Fig. 6. Again, the treatment pressures were high for this small-volume treatment, reaching a value of 1,100 psi [7.6 MPa] above the initial closure stress as shown in Fig. 6a. The log/log effective-treatment-pressure plot (Fig. 6b) shows an initially greater-than-expected exponent of 0.32, as opposed to the value of 0.26 expected for this rheology (n'=0.46; k'=0.02 lbf-sec$^{n'}$/ft^2 [0.96 N·sec$^{n'}$/m^2]). Later in the

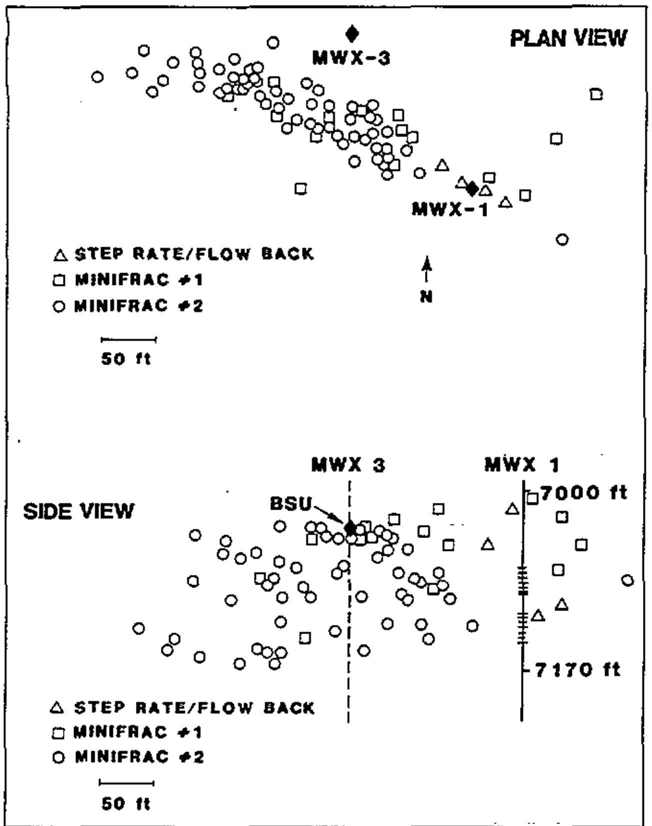

Fig. 7—Results of borehole geophones for minifractures.

treatment, the exponent decreases to 0.17, which may indicate some height growth out of zone. The temperature log shows some additional height over Minifracture 1; we estimate it to be 150 ft [46 m]. The Nolte pressure-decline analysis is shown in Fig. 6d. The modulus, leakoff height, and degradation are the same as Minifracture 1; the pump time was 88 minutes and the ISIP was 6,890 psi [48 MPa]. The analysis results in an estimated wing length of 420 ft [128 m] and a leakoff coefficient of 0.0007 ft/$\sqrt{\text{min}}$ [0.0002 m/$\sqrt{\text{min}}$]. The analysis of two shut-ins during this treatment gave an estimated leakoff coefficient of less than 0.001 ft/$\sqrt{\text{min}}$ [0.0003 m/$\sqrt{\text{min}}$]. These data indicated that fracture-length extension was occurring without excessive height growth even though the treatment pressures were abnormally high. Additionally, the low leakoff coefficient suggested that the nearby coals were not thieving excessive fracture fluid.

Minifracture Borehole Seismic Results. The results of the borehole seismic system have been reported by Hart *et al.*[5] and are shown in Fig. 7. Seismic signals created by the fracturing process were mapped by the geophones in Well MWX-3; the geophones in Well MWX-2 provided no clear data because of noise problems. The locations of origin of the seismic disturbances were mapped in 3D space and then projected on horizontal and vertical planes in Fig. 7 to show the fracture azimuth, height, and length. The measured fracture azimuth was N67°W for the one wing of the fracture from which the geophone in Well MWX-3 could accurately resolve locations. The height and length of this one wing were about 140 and 240 ft [43 and 73 m], respectively, for Minifracture 1 and 150 and 370 ft [46 and 113 m], respectively, for Minifracture 2. These numbers are very similar to the Nolte analysis results.

Postminifracture Cleanup and Well Tests

After completion of the minifracture tests, the well was cleaned for a week before cold weather necessitated a winter shutdown. During this week, 60% of the fluid load was recovered. During January, the well was flowed once a week for additional cleanup, and another 10% was recovered. Finally, the well was shut in for 2 months before the postminifracture well testing operations. In late March, testing began and an additional 22% of the initial load was recovered for a total of 92% (some of this may have been formation water).

Postminifracture testing[3] consisted of three consecutive drawdown periods at different rates, a shut-in period, and a final drawdown. The main purpose was to determine the effects of the treatment and the unpropped fracture on reservoir performance. No attempt was made to look for interference. We found that the productive capacity of the reservoir had decreased considerably, at least over the short times of these tests (25 days of testing). The formation capacity was estimated to be 0.64 md-ft [0.0002 md·m], a decrease of about 30%, and the AOF was about 200 Mcf/D [5665 m^3/d], as opposed to 250 Mcf/D [7080 m^3/d] prefracture. The unpropped fracture provided a relatively high, linear, conductive flow path with a fracture capacity, $K_f w$, of 75 md-ft [0.022 md·m] and a skin of −3.8. Apparently, the natural fractures had been damaged by the treatment, and test time was not sufficiently long to clean them, if they could be cleaned.

TABLE 2—TREATMENT DESIGN SCHEDULE*

Stage	Fluid	Amount (gal)	Sand Concentration (lbm/gal)	Sand (lbm)
1	Methanol	7,700	0	0
2	Apollo 40**	18,000	0	0
3	Apollo 35	3,000	1.5	4,500
4	Apollo 35	5,000	2.0	10,000
5	Apollo 35	6,000	3.0	18,000
6	Apollo 35	14,000	4.0	56,000
7	Apollo 25	18,000	5.5	99,000
8	Apollo 25	1,000	5.5	5,500
9	Water flush	8,764	0	0
	Total	81,464		193,000

*Courtesy of The Western Co.
**A 40-lbm/1,000-gal hydroxypropyl guar crosslinked with a titanium salt. Base fluid is a 3% KCl water with ½-gal/1,000-gal bactericide.

Hydraulic Fracture Design

The design of the second phase—the main hydraulic-fracture treatment—was influenced by several considerations. First, we wanted to optimize propped fracture length with respect to sand reservoir size. The extent of Zone 3 was probably 200 to 500 ft [61 to 152 m]; the extent of Zone 4 was unknown. We found no reasons for creating a fracture with a propped length greater than 500 ft [152 m]. Second, we were concerned about the high treatment pressures and preferred keeping the viscosities, flow rates, and volumes low to minimize the pressure. Third, we had no information on remote lenses (not intersected by the wells) and we were concerned about the effects of the coals on the treatment and production; this favored a small treatment. Fourth, the fracture diagnostics could only "see" about 400 ft [122 m], so much longer fractures would be difficult to diagnose.

Fracture height for the design models was uncertain because we had broken through the known upper barrier, yet we did not experience excessive out-of-zone growth. This is probably because the upper barrier significantly reduced fracture width there and acted as an efficient flow restriction. Because of these complications, we assumed a constant fracture height of 200 ft [61 m] for design purposes (this is based on the minifracture results). A gross leakoff coefficient of 0.00065 ft/$\sqrt{\text{min}}$ [0.0002 m/$\sqrt{\text{min}}$] for a full 200-ft [61-m] height was calculated from the minifracture results. Rock and reservoir properties are the same as before.

The results of this treatment are shown in Table 2. The crosslinked water-based fluid system, Apollo, was used and was staged from a concentration of 40 lbm/1,000 gal [4.8 kg/m^3] in the pad to 25 lbm/1,000 gals [3 kg/m^3] in the final proppant-carrying stage (all water is 3% KCl). For analyses requiring rheological data, the 35-lbm/1,000-gal [4.2-kg/m^3] gel at a residence time of 1 hour and temperature of 193°F [89.4°C] was considered average. Under these conditions, $n'=0.78$ and $k'=0.0061$ lbf-sec$^{n'}$/ft^2 [0.29 N·sec$^{n'}$/m^2]. Because of the high temperatures, breaker was

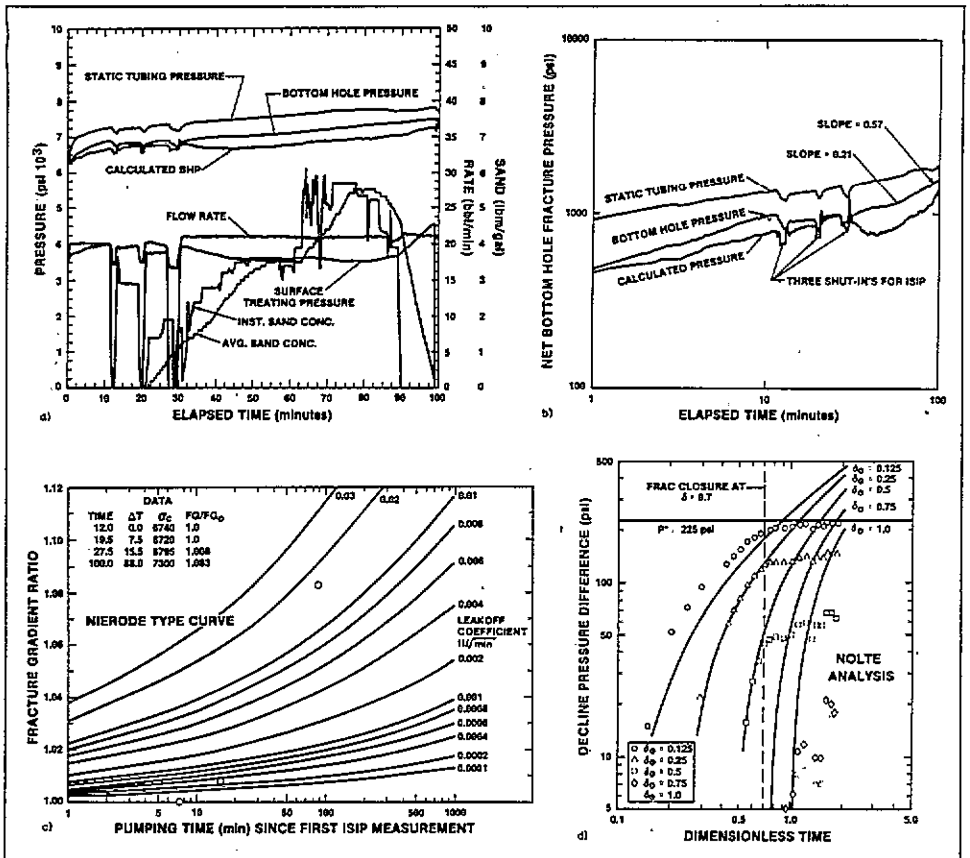

Fig. 8—Results of the Phase 2 stimulation.

added only in Stages 7 and 8 in concentrations of 0.25 to 0.5 lbm/1,000 gal [0.03 to 0.06 kg/m^3]; the addition of breaker in the earlier stages would have reduced viscosity sufficiently that sand fall-out would have been expected before the slurry reached the fracture extremities. Because of the success with fluid recovery in the minifractures, a methanol prepad was again used.

Sand concentrations were staged up to 5.5 lbm/gal [660 g/m^3], the maximum that we felt confident of being able to inject at rates of 20 bbl/min [0.053 m^3/s]. This results in an average design concentration in the fracture of about 1 lbm/ft^2 [4.9 kg/m^2]. A 20/40-mesh sand was used for all stages except the final one (Stage 8), in which 12/20 mesh was used for a tail-in. A radioactive-sand tag was used in the entire job; iridium 192 was used in the first half and iodine 131 in the last half of the treatment. Sufficient sand concentrations were used so that if the fluid broke before final closure, the resultant sand bank would fill both channel sands. Ammonium thiocyanate in a concentration of about 100 ppm was used as a fluid tag.

We planned to perform three shut-ins during pad pumping to estimate the leakoff coefficient using Nierode's[15] analysis, a short rate test (15 bbl/min [0.04 m^3/s]) during the pad to see the effect on treatment pressure, and a long postfracture shut-in to obtain pressure decline data.[13] We had the same diagnostic techniques as used in the minifractures, as well as a treatment monitoring vehicle for calculating BHP from surface injection conditions and extended real-time data-monitoring capabilities.

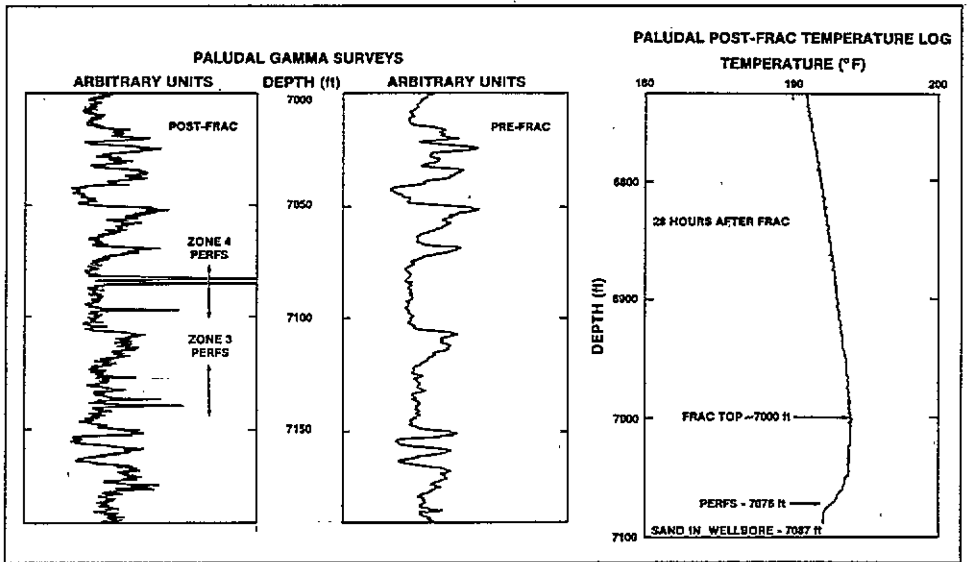

Fig. 9—Postfracture survey results.

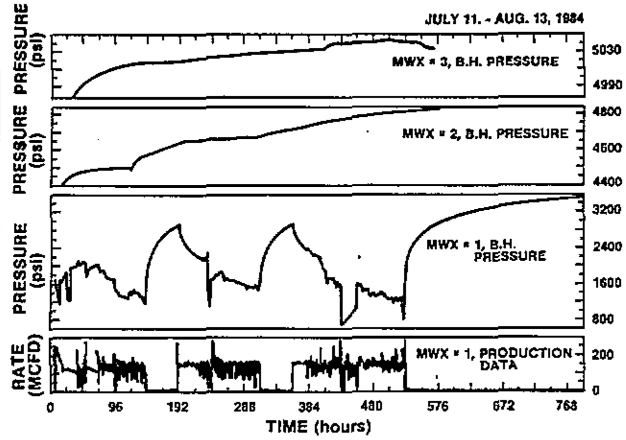

Fig. 10—Postfracture well test data.

Phase 2 Hydraulic Fracture Experiment

The Phase 2 hydraulic fracture was conducted in early May 1984. The well configuration consisted of 7-in. [18-cm] casing with a bridge plug at 7,200 ft [2195 m] and 2⅞-in. [7.3-cm] tubing landed open-ended at 6,750 ft [2057 m]. The pressure and temperature transducers were again in the tubing at 6,700 ft [2042 m] while we pumped down the annulus. Surface data included casing treatment pressure, static-tubing pressure, flow rate, sand concentration, base gel viscosity, and surface fluid temperature.

On the treatment day, the borehole geophones were lowered in Wells MWX-2 and MWX-3, oriented, and rechecked. KCl water (3%) was circulated down the annulus to remove gas in the well, and the 7,700 gal [29 m^3] of methanol were spotted in the annulus. Finally, the pressure and temperature tools were lowered and stabilized and the treatment begun.

Only one problem occurred during the treatment, and this was a result of problems with the BHP processor. It began to malfunction, and we were forced to shut in for about 40 minutes after pumping 163 bbl [26 m^3]. (Only methanol was in the formation at this point.) Once the problem was repaired, the treatment continued as planned. However, this unplanned shut-in probably resulted in a leakoff of much of the methanol in the near-wellbore region and in considerable viscosity degradation of the pad fluid that was sitting in the hot wellbore.

The results from the treatment are shown in Fig. 8. This includes the actual treatment data in Fig. 8a, the Nolte-Smith analysis in Fig. 8b, the Nierode analysis in Fig. 8c, and the Nolte pressure decline analysis in Fig. 8d. The difference in the three BHP measurements is a result of offsets in the three curves so that they could be distinguished. The curve labeled BHP is from the BHP gauge, is corrected to the top of the perforations, and is not offset. Treatment pressures reached about 1,500 psi [10 MPa] above closure stress during the job.

The Nolte-Smith fracture-pressure analysis shows a small slope (0.21) for the first half of the treatment, but then an increasing slope (to 0.57) the final half of the treatment. We were concerned that this was a sign of impending screenout. The three shut-ins during the pad and the final shut-in were used for the Nierode analysis. The initial data showed a low fluid-loss coefficient (the accuracy of those low points is questionable), but the final shut-in indicates a much greater fluid loss. Whether this is real in the sense that much greater fluid loss occurred at late times (possibly into the natural fractures) or whether there is some other explanation is uncertain.

The Nolte analysis provided our most interesting look at fracture behavior. Attempts to fit the pressure-decline data to the type curve were unsuccessful until we realized that something unusual occurred at a dimensionless time of 0.7 (because the pump time was 100 minutes, this is 70 minutes after shut-in). The pre-0.7 data can be fit nicely, while the post-0.7 data flatten significantly. We interpret this as initial fracture closure on the proppant, at least near the wellbore. The only way this could occur so early was if the gel broke, the sand fell to the bottom of the fracture, and any additional incremental leakoff would then result in closure of the bottom of the fracture on the proppant. Using the early data for the analyses, we obtain a wing length of 520 ft [158 m] and a leakoff coefficient of 0.0012 ft/$\sqrt{\text{min}}$ [0.0004 m/$\sqrt{\text{min}}$] if the height is 180 ft [55 m], or values of 420 ft [128 m] and 0.0015 ft/$\sqrt{\text{min}}$ [0.0005 m/$\sqrt{\text{min}}$] if the height is 200 ft [61 m]. The fluid efficiency in either case is 74%. Additional parameters for this analysis are a leakoff height of 80 ft [24 m], an ISIP of 7,300 psi [50.3 MPa], and a degradation exponent of 1.0.

The postfracture surveys were not very helpful in defining the fracture height, as shown in Fig. 9. We had trouble lowering the temperature tool into the zone because of sand fill, and we have, at best, a gross estimate of fracture top. The gamma survey only showed radioactive sand in the perforated interval and thus gave no indication of fracture height. Furthermore, the borehole geophones were plagued by high noise levels during this treatment, and only a few clear seismic signals were obtained. All that can be said about these data is that fracture azimuth was approximately the same as that of the minifractures, and the few signals that were obtained all fell within a 200-ft [61-m] height window. However, the accuracy of some of these points may have been poor.

Postfracture Cleanup

After completion of the treatment, the well was opened to clean up and produce back as much of the fracture fluid as possible. Recovery in the first few days was more than 50% of the total injected volume, but additional water recovery was much slower. Problems with sand in the wellbore, a stuck packer, and the wellhead and choke resulted in several shut-in periods and the circulation of water several times. These may have hampered the cleanup process somewhat. Over the next 4 weeks, additional water recovery was poor, and the well produced less than 50 Mcf/D [1416 m^3/d]. Furthermore, it showed no signs of improving.

Several buildups over this period seemed to indicate that the fracture was very short (10 ft [3 m]), as if it were clogged or bridged. Continuous returned fluid samples were taken, and analysis of the organics indicated molecular weights on the order of 2×10^6. We were afraid that the minimal amounts of breaker that we used to ensure good proppant transport may have resulted in inadequate breaking of the gel (at least over this period of a few weeks) and possibly a gel plug existed in the near-wellbore region. Because schedule concerns would not allow us to wait indefinitely for the gel to break completely by formation temperature, we proceeded with a remedial breaker treatment in an attempt to break any gel plug and to ensure conductivity in the fracture.

Remedial Treatment. The remedial treatment consisted of 6,500 gal [25 m^3] of 3% KCl water with 135 lbm/1,000 gal [16 kg/m^3] of ammonium persulfate breaker plus 1,000 gal [3.8 m^3] of 3% hydrogen peroxide. This 7,500-gal [28-m^3] total volume was sufficient to fill the fracture porosity with excess. It was injected at sufficiently low rates (1 to 2 bbl/min [0.002 to 0.005 m^3/s]) to keep the BHP below 6,000 to 6,200 psi [41 to 43 MPa] and thus not open the fracture. This treatment was completed with no problems, but we saw an immediate 1- to 2-psi [7 to 14-kPa] response with a BHP gauge in Well MWX-2. Whether this was an actual interference through connected permeability or a poromechanical response to the pressurized crack is uncertain; both are possible.

The load water from the remedial treatment was recovered within a week, and fluid recovery after this treatment was two to three times better than before. Water samples showed that the molecular weights of the polymer were now less than 200,000, down from about 1,000,000. Unfortunately, while this treatment cleaned up the gel residues, it also resulted in the formation of large amounts of iron oxide precipitates because of the reactive nature of the chemicals. Most of these were from reaction with the tubing and casing; however, core studies after the fact showed a 40% reduction in permeability and more than doubled cleanup times. Permeability reduction in an artificially created fracture in the core was about 90% with cleanup times increasing about two orders of magnitude. We may have exchanged one problem for another. Additionally, ionic analyses of the returned fluids indicated that we were producing increased amounts of formation waters, possibly from the coals.

TABLE 3—POST-FRACTURE WELL-TEST DATA*

Time (days)	Production Rate (Mcf/D)	BHP (psi)	Cumulative Gas (Mcf)
0.5	225	1,307	150
1.0	114	1,514	193
1.5	107	1,971	257
2.0	64	2,071	296
2.5	120	1,958	369
3.0	171	1,932	437
3.5	147	1,726	524
4.0	171	1,504	597
4.5	157	1,319	670
5.0	151	1,400	741
5.5	150	1,327	817
5.87	146	1,222	852
6.02	0	2,004	
6.06	0	2,067	
6.13	0	2,145	
6.28	0	2,281	
6.43	0	2,393	
6.58	0	2,488	
6.73	0	2,566	
7.05	0	2,698	
7.20	0	2,748	
7.36	0	2,792	
7.51	0	2,831	
7.65	0	2,877	
7.80	0	2,901	
7.9	182	2,847	862
8.5	142	2,439	953
9.0	159	2,231	1,047
9.5	120	2,149	1,108
10.0	154	1,702	1,196
10.5	81	1,860	1,233
11.0	126	1,702	1,284
11.5	155	1,658	1,389
12.0	158	1,580	1,458
12.5	152	1,515	1,533
13.0	120	1,521	1,597
13.11	0	2,056	
13.18	0	2,158	
13.29	0	2,265	
13.36	0	2,329	
13.44	0	2,385	
13.51	0	2,435	
13.58	0	2,481	
13.81	0	2,585	
14.25	0	2,766	

TABLE 3—POST-FRACTURE WELL-TEST DATA* (continued)

Time (days)	Production Rate (Mcf/D)	BHP (psi)	Cumulative Gas (Mcf)
14.55	0	2,848	
14.99	0	2,892	
15	145	2,764	1,605
15.5	152	2,469	1,688
16.0	151	2,285	1,755
16.5	171	2,265	1,827
17.0	189	1,738	1,929
17.5	164	1,708	2,004
18.0	173	1,540	2,076
19.0	159	1,556	2,190
20.0	152	1,384	2,346
21.0	162	1,249	2,492
21.93	186	864	2,641
21.96	0	1,019	
21.98	0	1,733	
22.03	0	1,948	
22.08	0	2,077	
22.21	0	2,275	
22.32	0	2,365	
22.54	0	2,510	
22.78	0	2,615	
23.01	0	2,705	
23.24	0	2,778	
23.59	0	2,861	
24.05	0	2,952	
24.49	0	3,022	
24.93	0	3,078	
25.38	0	3,124	
25.80	0	3,164	
26.46	0	3,216	
27.13	0	3,261	
27.79	0	3,299	
28.53	0	3,338	
29.50	0	3,386	
30.70	0	3,438	
31.44	0	3,466	
32.45	0	3,501	

*Water production less than 2 B/D; no condensate.

TABLE 4—PALUDAL TEST PARAMETERS

Reservoir parameters	
Initial pressure, psi	5,400
Temperature, °F	210
Gas specific gravity	0.67
Net porous thickness, ft	26
Average porosity, %	10.2
Average permeability, μd	36
Average water saturation, %	46
Average core permeability, μd	1
Completion parameters	
Perforation depths, ft	7,076 to 7,100
	7,120 to 7,144
Casing ID, in.	6.184
Tubing ID, in.	2.441
Packer depth, ft	7,050
Bridge plug depth, ft	7,200
Pressure buildup wellbore volumes, bbl	
Buildup 1 and 2	46
Final buildup with downhole closure	6

The well still did not flow readily, and we continued cycling the well to produce as much fluid as possible. Throughout this cleanup phase, the well configuration consisted of open-ended tubing situated just above the perforations. Gas flow rates were too low to give us lift up the tubing. After 1 month of gradual cleanup, we changed the well configuration and inserted a packer with tubing extending below the perforations. The packer gave us better control of BHP (we find that we need to maintain at least 1,000-psi [7-MPa] BHP to keep gas flowing in these formations), and the long tubing tail provided a method to drain the maximum amount of fluid from the fracture and wellbore. We immediately recovered about 50 bbl [8 m^3] of liquid and obtained gas flows in excess of 100 Mcf/D [2832 m^3/d]. At this point, the total recovery of fracture fluid was somewhat less than 70%, while the recovery of all fluids put in the well since the treatment was more than 80%.

Postfracture Well Testing

We continued to flow Well MWX-1 while we prepared the other two wells for another interference test.[3] In mid-July 1984, this test was started, and the important data are shown in Fig. 10 and Table 3. Specific reservoir and completion data are given in Table 4. The testing consisted of three drawdowns with two interspersed buildup pulses and a long, final buildup in Well MWX-1. The maximum sustainable flow rate (AOF) was about 170 Mcf/D [4814 m^3/d], down from the previous flow tests. No clear indication of interference was seen in Well MWX-2 or MWX-3 during these tests. While some pressure disturbances can be seen in Fig. 10, none of these are correlatable with flow or shut-in periods in Well MWX-1 on a constant delta-time basis; i.e., if we see a pressure response as a result of one pulse at some delayed time Δt, we should see another pressure response as a result of the next pulse at approximately the same Δt after the pulse. No such behavior is obvious.

To interpret these results, both homogeneous and dual-porosity reservoir simulators were used. We assumed that the far-field in-situ permeability was 36 μd because of the natural-fracture system, but the natural-fracture system near the induced hydraulic fracture was plugged, and the permeability in this damaged region was equal to the matrix permeability, about 2 μd. We proceeded to match the Well MWX-1 BHP data by varying the hydraulic-fracture length and the thickness of the damaged zone around the fracture. A suitable match (see Ref. 3) was found with a damage thickness of 9 ft [2.74 m] on both sides of the fracture and an effective fracture wing length of 75 ft [23 m]. This short length could be a result of either a short fracture or a narrow reservoir channel; the two cases are indistinguishable. Thus, our best match of the well test data shows that we further damaged the existing natural-fracture system, as we also did in the minifractures. Because we believe from the minifracture results that we had a fracture longer than 75 ft [23 m], the channel reservoir size appears to be only about 150 ft [46 m] in total permeable width where the fracture intersects it.

We expect that the reservoir damage would have continued to clean up with much longer production times, but the length of our test time was constrained by other factors. Nevertheless, such long cleanup times will be a problem for any operator.

Final Production Tests After a Long-Term Shut-In

Testing of these paludal sands was suspended in mid-Aug. 1984, while we tested other zones uphole. In late March 1986 (20 months later), however, an opportunity arose to retest these zones to evaluate any time dependence of the suspected damage. The zone was flow tested for 7 weeks with an initial rate of 420 Mcf/D [11.9 m^3/d], a cumulative produced volume of 15.8 MMscf [447×10^3 std m^3], and an average rate of 320 Mscf/D [9060 std m^3/d]. No liquids were produced initially, but after 5 days, water production started, increased rapidly to about 35 B/D [5.6 m^3/d], and eventually totaled 860 bbl [137 m^3].

These results suggest that the damage after the fracture is reversible and is probably caused by water and gel blockage of the natural fractures. Over the long shut-in, the gel may have degraded further, and imbibition of the water into the matrix rock probably cleared the natural fractures of most water and dehydrated any remaining gel. When production was resumed, gas production through the natural fractures was no longer hindered, and flow rates were much closer to the expected values.

Discussion

Lens Morphology. The final well test analysis showed that the intersection of the fracture length and the reservoir was only about 150 ft [46 m]. Because we believe the fracture was much longer than this (the minifractures were about 400 ft [122 m] and the Nolte analysis gave a minimum length of 400 ft [122 m] for the main treatment), the probable reason for this result is a narrow channel width. This is consistent with widths measured in outcrop by Lorenz[2] and shows the importance of such studies for a complete evaluation of stimulation and well test data, as well as for treatment design and for production and economic forecasts.

Natural Fractures. A comparison of core and well test data leads us to conclude that the major flow paths are natural fractures and that the system must be fairly interconnected to show no sign of linear flow. Any well completion operations must be carefully designed to limit any damage to the natural-fracture system. We also find that these reservoirs will not produce unless a backpressure (in this case about 1,000 psi [7 MPa]) is maintained at the sand face. Branagan *et al.*[3] suggest that this may be a stress sensitivity of the natural-fracture system.

Interference. During the prefracture and postfracture well tests, no certain evidence of interference was found in the pressure data or even in the slopes of the pressure data. While this may have been masked somewhat by the pressure recovery occurring simultaneously in the interference wells (see Fig. 10), permeabilities of 36 μd and flow rates of 250 Mcf/D [7180 m^3/d] should have been sufficient to impart an observable superposed pressure response. Factors hampering communication are the thinning of Zone 3 at Well MWX-3, the lack of Zone 4 in Well MWX-2, and the fault in Well MWX-2. Even with these features, good sand connectivity should exist. We can only surmise that this lack of interference is a result of one of two things. Either the fracture networks are isolated and may not intersect all wells, or sufficient shale breaks exist that each well is in communication with an isolated reservoir. If the latter is true, analysis becomes extremely difficult.

Abnormal Treatment Pressures. During all fracturing tests in this zone, we observed very high pressures during the treatments. Several possible reasons exist for such high pressures. The first possibility is complex fracturing, as discussed by Medlin and Fitch[16] for other wells in the Mesaverde in the Piceance basin. The second possibility is that the fracture reached the lateral ends of the lens so that treatment pressures would need to increase substantially for excessive fracturing to occur in the higher-stress shales. The short, effective fracture lengths measured in well tests make this credible. The third possibility is backstresses caused by fluid leakoff, but this is typically a much smaller effect. The fourth possibility is the presence of high-stress stringers, possibly between the zones, that would reduce fracture widths and increase pressures somewhat. All these factors may have contributed to the pressure levels. Whatever the cause, high pressures can result in many deleterious effects; the most obvious one is wider, shorter hydraulic fractures.

Reservoir Damage. All the well test data support the premise of damage to the natural fractures as a result of the treatment. The important questions are why this damage occurs and why it is so hard to clean up. We believe that the degree of damage is in large part a result of the high treatment pressures. These high pressures may have either opened the intersecting natural fractures or forced the gel into them under such high differential pressures that production of these gels was difficult under normal reservoir conditions. This indicates that cleanup times will always be excessive when treatments are conducted in this environment with a water-based system. One good alternative is to use a foam fracturing system so the fractures are exposed to less water. Another alternative is not to fracture at all and accept the initial 250 Mcf/D [7080 m^3/d], or possibly to try a treatment, such as tailored pulse loading,[17] where the only intent is to obtain a good connection with the natural-fracture system.

Diagnostics and Analyses. After the minifractures, we were surprised at the similarity of the results of the borehole geophones, the temperature log, and the Nolte analysis. This agreement in independent diagnostic techniques gave us confidence in their accuracy. Additionally, the fracture azimuth determined during the treatment agreed with prefracture predictions obtained from core, log, and surface stress orientation measurements.[7] The data from the main treatment, while disappointing, produced consistent trends in fracture behavior.

Containment. We apparently had acceptable containment even though the treatment pressures were much higher than any barrier stress, so any barrier (particularly the top one) should have been penetrated. We attribute this to these high-stress layers acting as restrictions rather than absolute barriers. Because of the high stresses, fracture widths are much smaller in these layers, and thus, pressure drops become very large when we try to force fluid through them at any fast rates. Thus vertical growth occurs quite slowly. In addition, proppant may bridge in these narrow regions.

Coals. We had been concerned about the effect of the coals in the treatment and gas production, but no obvious deleterious developments seemed to occur. One positive effect was the high stress in the coal above Zone 4 (the highest stress in the paludal interval), which probably was a significant factor limiting height growth. No obvious loss of fracture fluid occurred because of the coals, but water production from the coals may have been partly responsible for the hindered cleanup.

Proppant Crushing. We designed the treatment with a sand proppant because we felt that a closure stress of 5,900 psi [40.7 MPa] combined with a minimum wellbore pressure of more than several hundred psi would result in acceptable conductivities for the sandpack, particularly with our formation permeabilities. With the cleanup problems and repeated blowdowns, however, we probably often had effective stresses on the proppant approaching the total closure stress. When combined with the cyclic fatigue loading, these high stresses may have resulted in much reduced conductivity. We suggest that in these situations the proppant should be overdesigned, at least near the wellbore.

Reversibility of the Damage. Our ability to produce this zone at much higher rates after the 20-month shut-in demonstrates that the damage is primarily liquid-induced (gel, water), as opposed to mechanical damage to the natural fracture system. Because the initial production after shut-in was dry, we can also deduce that imbibition of the fracture load water into the matrix pore volume was a positive factor because it cleared the natural fractures.

Conclusions

We have successfully completed a fracturing and testing experiment in the paludal zone of the Mesaverde. While the experiment was disappointing in terms of gas production, the primary objectives of understanding hydraulic-fracture behavior and reservoir characteristics in lenticular formations have been largely realized. Important considerations—such as lens morphology, reservoir characteristics, gas flow mechanics, fracture containment and lateral extension out of lenses, fracture fluid damage, and many others—have been addressed. We hope that the discussion of these topics and the recommendations that we have made will be helpful to other operators.

Acknowledgments

We thank Dave and Bill Holcomb of Smith Energy Services, and Larry Harrington, Lacy Lance, and Laddie Harp of The Western Co. for their help and suggestions during these experiments. Special thanks go to the CER field crew, whose hard work made many of these studies successful. We also thank Carolyne Hart for her diagnostic work, Gerry Kukal for his log analyses, and Clarence Raible and Bonnie Gall at the Natl. Inst. of Petroleum Energy Research for many of the laboratory analyses. Special core analyses were provided by Core Laboratories. This work was sponsored by the U.S. DOE's Western Gas Sands Subprogram, which is managed by Morgantown Energy Technology Center under Contract No. DE-AC04-76DP00789.

References

1. "Unconventional Gas Sources—Volume V: Tight Gas Reservoirs, Part I," Natl. Petroleum Council, Library of Congress Card Number 80-82488 (Dec. 1980) V.
2. Lorenz, J.C.: "Predictions of Size and Orientations of Lenticular Reservoirs in the Mesaverde Group, Northwestern Colorado," paper SPE 13851 presented at the 1985 SPE/DOE Symposium on Low Permeability Reservoirs, Denver, May 19–22.
3. Branagan, P. *et al.*: "Comprehensive Well Testing and Modeling of Pre and Post Frac Well Performance of the MWX Lenticular Tight Gas Sands," paper SPE 13867 presented at the 1985 SPE/DOE Symposium on Low Permeability Reservoirs, Denver, May 19–22.
4. Sattler, A.R.: "Integration of Laboratory and Field Data to Interpret Stimulation Results in Lenticular Tight Gas Sands," paper SPE 13891 presented at the 1985 SPE/DOE Symposium on Low Permeability Reservoirs, Denver, May 19–22.
5. Hart, C.M. *et al.*: "Fracture Diagnostics Results for the Multiwell Experiment's Paludal Zone Stimulation," *SPEFE* (Sept. 1987) 320–26.
6. Lorenz, J.C. *et al.*: "Determination of Widths of Meander Belt Sandstone Reservoirs from Vertical Downhole Data, Mesaverde Group, Piceance Creek Basin, Colorado," *AAPG Bulletin* (1985) 69, 710–21.
7. Teufel, L.W. *et al.*: "Determination of Hydraulic Fracture Azimuth by Geophysical, Geological, and Oriented Core Methods at the Multiwell Experiment Site, Rifle, CO," paper SPE 13226 presented at the 1984 SPE Annual Technical Conference and Exhibition, Houston, Sept. 16–19.
8. Randolph, P.L.: "Porosity and Permeability of Mesaverde Sandstone Core from the U.S. DOE Multiwell Experiment, Garfield County, Colorado," paper SPE 11765 presented at the 1983 SPE/DOE Symposium on Low Permeability, Denver, March 14–16.
9. Kukal, G.: "Multiwell Experiment Well Log Analysis of Paludal Interval," CER Report, Las Vegas (Oct. 1984).
10. Searls, C.A.: "The Multiwell Experiment Geophysics Program Final Report," Sandia Natl. Laboratories Report, SAND85-1013 (Sept. 1985).
11. Warpinski, N.R., Branagan, P., and Wilmer, R.: "In-Situ Stress Measurements at DOE's Multiwell Experiment Site, Mesaverde Group, Rifle, Colorado," *JPT* (March 1985) 527–36.
12. Lorenz, J.C. *et al.*: "Fracture Characteristics and Reservoir Behavior of Stress-Sensitive Fracture Systems in Flat-Lying Lenticular Formations," paper SPE 15244 presented at the 1986 SPE Unconventional Gas Technology Symposium, Louisville, May 18–21.
13. Nolte, K.G.: "Determination of Fracture Parameters from Fracturing Pressure Decline," paper SPE 8341 presented at the 1979 SPE Annual Technical Conference and Exhibition, Las Vegas, Sept. 23–26.
14. Nolte, K.G. and Smith, M.G.: "Interpretation of Fracturing Pressures," *JPT* (Sept. 1981) 1767–75.
15. Nierode, D.E.: "Comparison of Hydraulic Fracture Design Methods to Observed Field Results," paper SPE 12059 presented at the 1983 SPE Annual Technical Conference and Exhibition, San Francisco, Oct. 5–8.
16. Medlin, W.L. and Fitch, J.L.: "Abnormal Treatment Pressures in MHF Treatments," paper SPE 12108 presented at the 1983 SPE Annual Technical Conference and Exhibition, San Francisco, Oct. 5–8.
17. Cuderman, J.F.: "Tailored-Pulse Fracturing in Cased and Perforated Borehole," paper SPE 15253 presented at the 1986 SPE Unconventional Gas Technology Symposium, Louisville, May 18–21.

SI Metric Conversion Factors

°API	141.5/(131.5+°API)		=	g/cm^3
bbl	× 1.589 873	E−01	=	m^3
ft	× 3.048*	E−01	=	m
ft^3	× 2.831 685	E−02	=	m^3
°F	(°F−32)/1.8		=	°C
gal	× 3.785 412	E−03	=	m^3
in.	× 2.54*	E+00	=	cm
lbm	× 4.535 924	E−01	=	kg
psi	× 6.894 757	E+00	=	kPa

*Conversion factor is exact.

SPEFE

Original SPE manuscript received for review May 19, 1985. Paper accepted for publication March 14, 1986. Revised manuscript received March 25, 1987. Paper (SPE 13876) first presented at the 1985 SPE/DOE Low Permeability Gas Reservoirs Symposium held in Denver, May 19–22.